Influence on Grinding Force Distribution in Setting Depth of Cut Variations of Cemented Carbide with Vertical Face Grinding

Ryo KOMATSUBARA [1,a *], Takanori FUJIWARA [1,b], Takashi TSUJINO [2,c]
Hiroyuki KODAMA [1,d], Takashi ONISHI [1,e] and Kazuhito OHASHI [1,f]

[1]Graduate School of Natural Science and Technology, Okayama University,

[2]Graduate School of Natural Science and Technology, Okayama University (Currently at TOYOTA MOTOR CORPORATION)

3-1-1 Tsushima-naka, Kita-Ward, Okayama city, Okayama, 700-8530, JAPAN

[a]prto36jq@s.okayama-u.ac.jp, [b]takanori@crc.okayama-u.ac.jp, [c]pilk9z2e@s.okayama-u.ac.jp,

[d]h-kodama@okayama-u.ac.jp, [e]pte487ph@okayama-u.ac.jp and [f]k-ohashi@okayama-u.ac.jp

Keywords: Cup type electroplated diamond grinding wheel, Cemented carbide, Grinding force, Grinding force distribution, Surface integrity of grinding wheel working surface

Abstract. Cemented carbide is very hard and suitable for molds and tools, although because of its high hardness and strength, both high precision and high efficiency processing methods have not been established yet. Then in this paper, we carried out this research in order to establish highly accurate grinding technology, also to clarify the grinding mechanism. In the face grinding of the cemented carbide is carried out with the parameter of the wheel setting depth of cut while constant feed rate of wheel head. This is a distribution of where and how much load is applied to the grinding wheel working surface during a grinding process, which has a pressure dimension. And it is measured by the difference of rise up part of a grinding force when the grinding wheel re- starts to interfere with the cemented carbide which was transcribed a wheel envelope shape. As the setting depth of cut with a cup type diamond grinding wheel increases, it was made clear by grinding experiment that the peak value of grinding force distribution increases and a peak width slightly became broad, and an adhesion of the cemented carbide and drop off of grains were started in the peak area.

Introduction

By using a cup type electroplated diamond wheel, it is possible to easily carry out a face grinding by using a machining center. However, there is not much research on the face grinding [1, 2]. Such as the study on abrasive wear of cup type grinding wheel [3], and development of a suction type tool that performs wet processing by sucking the grinding fluid supplied from an external nozzle into the interference area and so on are reported [4]. And a grinding force distribution is introduced to analysis of a grinding force in face grinding of cemented carbide, and by a difference of grinding part of wheel leads to a difference of grinding force distribution's variation [5]. Furthermore, an increase of a feed rate becomes an increase of a grinding forth and slightly decrease of the grinding forth distribution's peak value, while a peak width of the grinding force distribution becomes broad, in a condition under a constant setting depth of cut and feed rate variations [6]. In this research, using both a cup type electroplated diamond grinding wheel and a brazed diamond grinding wheel, with a shape with a slope attached to an outer circumference. It keeps a feed velocity of a grinding wheel head, by varies the setting depth of the cut constant for each pass and performing the face grinding of the cemented carbide is done The grinding force and the grinding force distribution generated on the working surface of the grinding wheel, the amount of both stock removal and residual stocks and the change in the surface roughness were experimentally analyzed.

Experimental method

Figure 1 shows the experimental apparatus of this study. We give the feed rate of 100mm/min in the X-axis direction to a cup type diamond grinding wheel with a slope of 1.5mm height per 3mm width at an outermost periphery which is attached to a rotating spindle of a vertical axis of the grinding center. Then it performs 1 pass grinding of 10 mm wide cemented carbide block workpiece. The main experimental conditions are shown in Table 1. As the interference between the grinding wheel and the workpiece is prepared by the several times of zero cut pass. And the feed rate of the wheel head is fed to the cup type grinding wheel vertically to the workpiece with settled grinding depth of cut. Then it performed spark out grinding for 30 seconds and transfer the envelope shape of the peripheral part of the grinding wheel, and traverse motion is fed again. The grinding fluid is supplied at a predetermined amount at two ports, one is from grinding fluid supply ports at bottom of the wheel both which penetrate the grinding wheel inner and outer part of the wheel working surface, and the other is from an external nozzle attached in the direction of movement of the grinding wheel. The workpiece is held by precision vice attached to piezoelectric tool dynamometer.

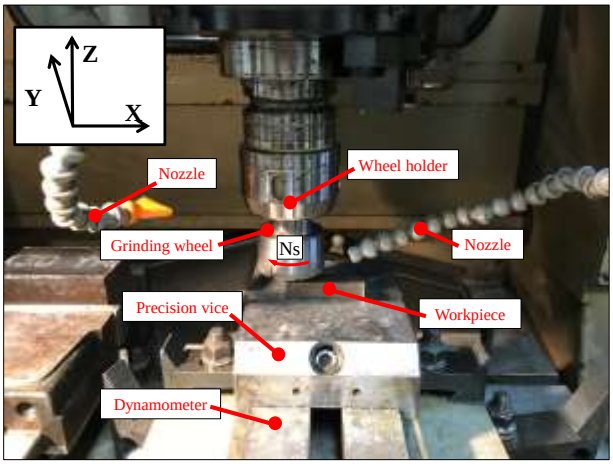

Fig. 1 Grinding test equipment apparatus

Table 1 Grinding conditions

Grinding wheel	Cup type diamond grinding wheel（#50 electro plated and #80 brazed, ϕ 50）
Workpiece	Cemented carbide G5（HV=1250）
Grinding wheel rotational speed	N_s = 2500rpm
Grinding wheel feed speed	V_f = 100mm/min
Grinding wheel cutting depth	Δ = 100, 200, 400 and 800μm/pass
Grinding fluid flow rate	G_f = 8.5L/min

Grinding wheel

In this study, two types of the grinding wheel are used, one of them is an electro plated #50 SD grinding wheel, and the other is a brazed single layer #80 SD grinding wheel. Fig 2 show appearances of grinding wheel, and Fig 3 show cross sections of the grinding wheel. Both wheel have masked surface which have no diamond grain.

Calculation method of grinding force distribution

Figures 4 and 5 show the grinding force distribution model and the calculation method of grinding force distribution [5]. Firstly, when the grinding wheel and the workpiece interfere by the distance b in the grinding wheel feed direction, define the resistance generated per unit length as Δp_1. At this time, since the grinding resistance P_1/ℓ per unit width is an integral value of the bar graph in Fig. 4, so it can be expressed as

$$P_1/\ell = \Delta p_1 \times b. \quad (1)$$

Secondly, the grinding wheel is sent for a minute distance b. In this case, it is considered that the amount of grinding of the outermost portion does not always change, so the force distributionΔp_1 per unit width also does not change in the outermost portion area. Therefore, if the force distribution newly generated in the b-2b region isΔp_2, the grinding resistance P_2/ℓ per unit width is as follows.

$$P_2/\ell = P_1/\ell + \Delta p_2 \times b. \quad (2)$$

Thirdly, from the above, considering the (n-1) to (n) regions, the grinding force distribution per unit width in this region is as follows.

$$\Delta p_n = (P_n - P_{n-1}) / (b \cdot \ell) . \quad (3)$$

Therefore, the grinding force distribution can be calculated by the consecutive difference between the grinding force values. Furthermore, the grinding force distribution Δq_n is given by this equation.

$$\Delta q_n = (Q_n - Q_{n-1}) / (b \cdot \ell) . \quad (4)$$

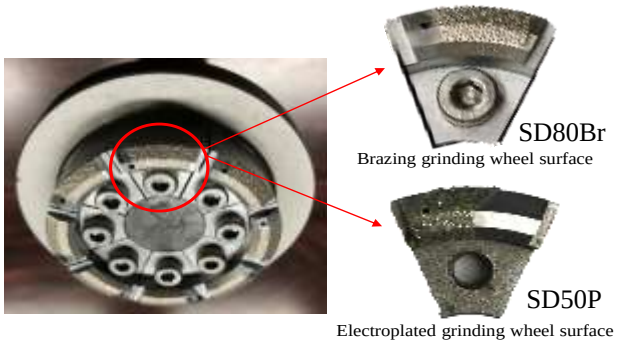

Fig 2 Grinding wheel apparatus

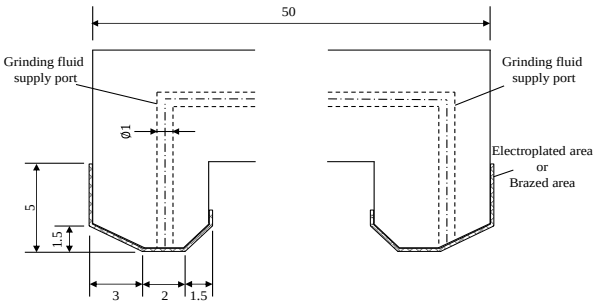

Fig 3 Cross section of grinding wheel

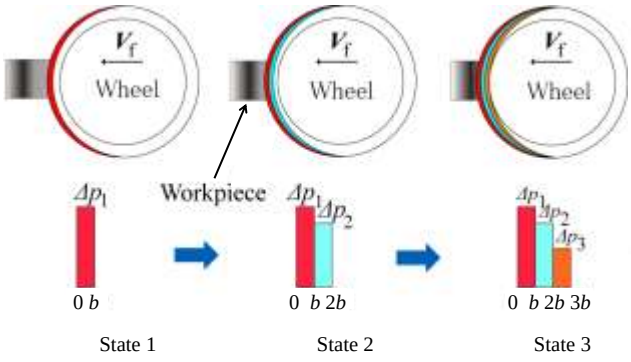

Fig 4 Grinding force distribution model

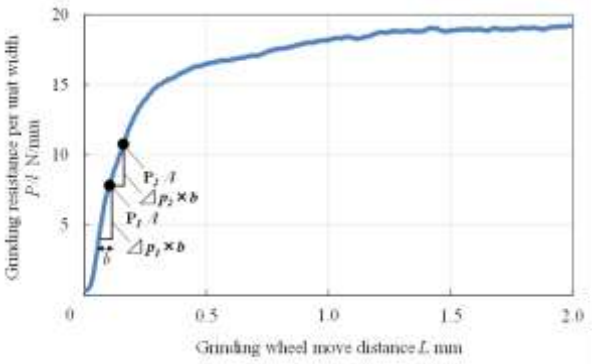

Fig 5 Calculation method of grinding force distribution

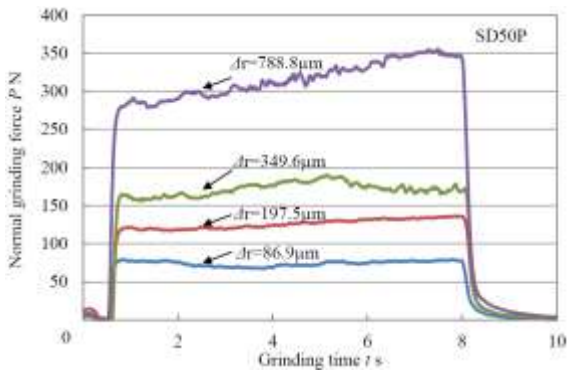

Fig 6 Variations of normal grinding force with SD50P

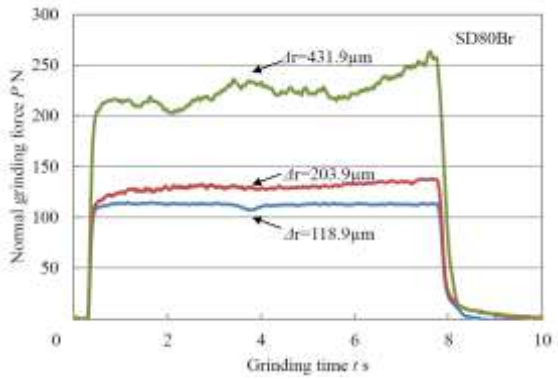

Fig 7 Variations of normal grinding force with SD80Br

Normal grinding force variation

Fig 6 show the variations of the normal grinding force by the SD50P wheel. Below the setting

depth of cut is 400μm, a steady grinding state is occurred, on the other hand if the setting depth of cut is over 400μm, the steady grinding state is not occurred. Every variation has a momently rise up of the normal grinding force immediately after re-approach to the spark out grinding surface. From the rise up part of the grinding force, the grinding force distribution is calculated as mentioned before.

In the case of SD80 brazed wheel, Fig 7 show variations of the normal grinding force. Below the setting depth of cut is 200μm, the steady grinding state is occurred. But the setting depth of cut is over 400μm, the steady grinding state is not occurred. And the setting depth of cut is over 800μm, the wheel is destroyed by the grinding force. Furthermore, a number of simultaneously working grains are less than the SD50P wheel, so the chip size becomes larger, and the actual load of individual grains become larger, then the grinding forces might become larger than the SD50P wheel.

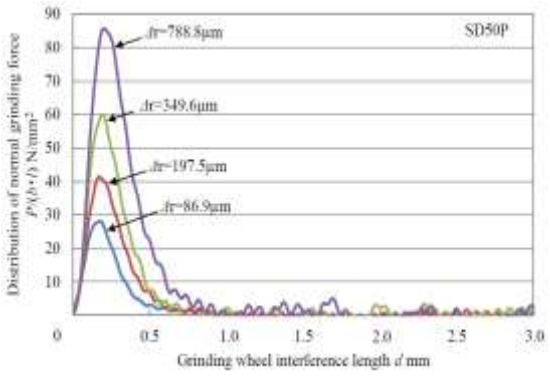

Fig 8 Variations of normal grinding force distribution with SD50P

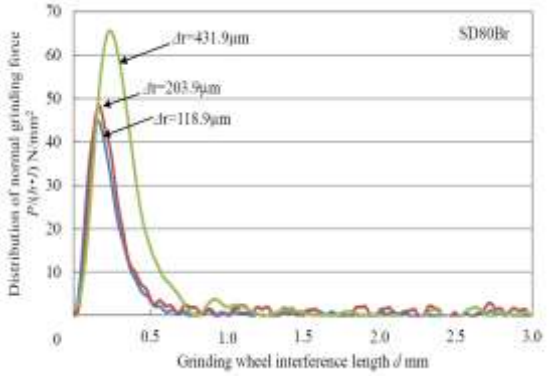

Fig 9 Variations of normal grinding force distribution with SD80Br

Grinding force distribution

Fig 8 show variations of the normal grinding force distribution Δp_n of the SD50P wheel. The peak value increase with the increase of the setting depth of cut. It is caused by the load of the grain becomes large with the increase of the depth of cut. And the peak width almost the same with the increase of the setting depth of cut. The mean grain size is 297μm, so the interference area of the wheel is located almost the bottom part of the wheel. It is showed that the area which loads the grinding force is located 0.5mm from the beginning part of the wheel interference area. The beginning point of the grinding force distribution's rise up is advanced with the increase of the setting depth of cut.

Fig 9 show the variations of Δp_n of the SD80Br wheel. The actual values of the grinding force distributions are the same in the case of the SD50P wheel. The mean grain size of the SD80Br wheel is 177 μm, so the interference area of the wheel is also located almost the bottom part of the wheel. The grinding force distributions of SD80Br wheel are larger than the case of the SD50P wheel, because of the large chip size caused by less amount of grains.

Surface integrity of wheel working surface and grinding force distribution

Fig 10 show the SEM photograph of the wheel working surface and the grinding force distribution by the SD50P wheel in the real setting depth of cut Δ_r=349.6μm, which occurs the steady grinding state. Upper left black circle is an outer peripheral grinding fluid support port, and upper part is the outer peripheral slope of the wheel working surface. The internal part of the grinding fluid supply port is matched to the beginning of the wheel bottom surface. The workpiece material is adhered to the bottom part of the grinding wheel, and the beginning position of adhesion is nearly matched to the beginning part of the grinding force distribution's rise up. It is assumed that the adhesion is generated because the grinding fluid supply port is located outer part of the wheel bottom, so the grinding fluid is lucked by the centrifugal force, then the cooling ability is degraded around the bottom of the grinding wheel.

Fig 11 show the SEM photograph of the wheel working surface and the grinding force distribution by the SD80Br wheel in the setting depth of cut Δ_r=203.9μm which occurs the steady grinding state. Because of the grain arrangement is coarser, the cooling ability of the grinding fluid might be maintained, and so the adhesion of the workpiece material is suppressed. Furthermore, the grains are dropped off around the peak width of the grinding force distribution, and the base metal of the wheel interferes to the workpiece.

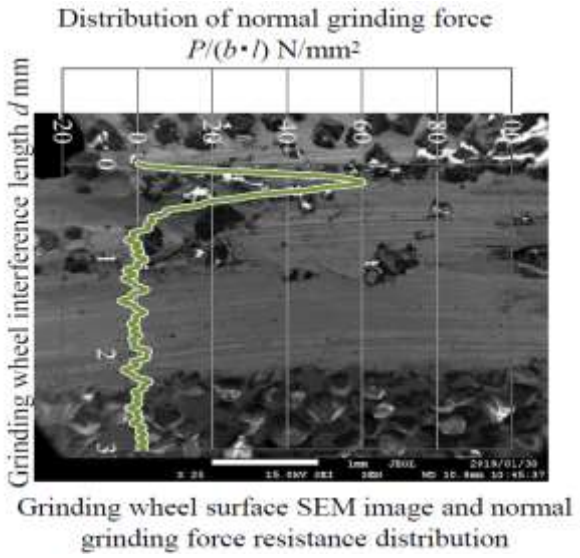

Fig 10 SEM photograph and grinding force distribution with SD50P (Δ_r=349.6μm)

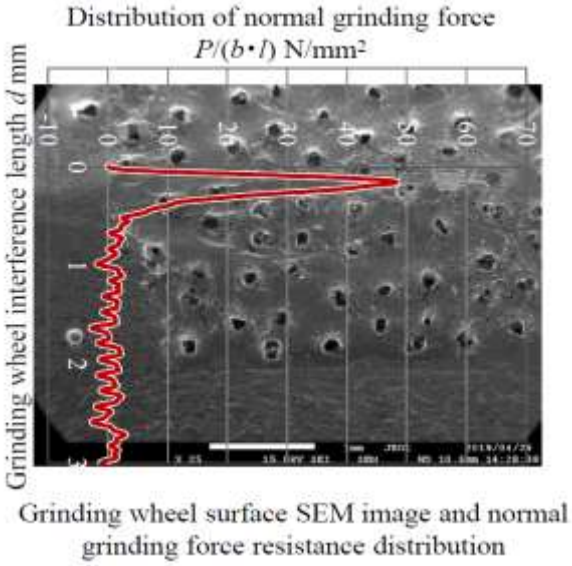

Fig 11 SEM photograph and grinding force distribution with SD80Br (Δ_r=203.9μm)

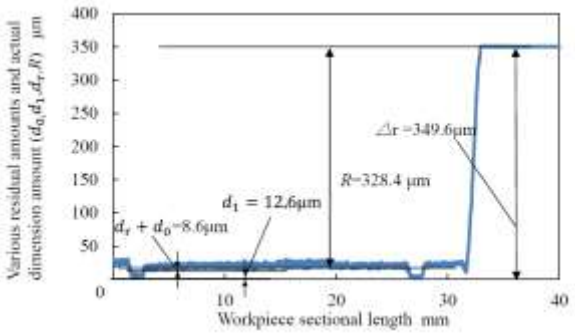

Fig 12 Variations of residual amount and stock removal with SD50P (Δ_r=349.6μm)

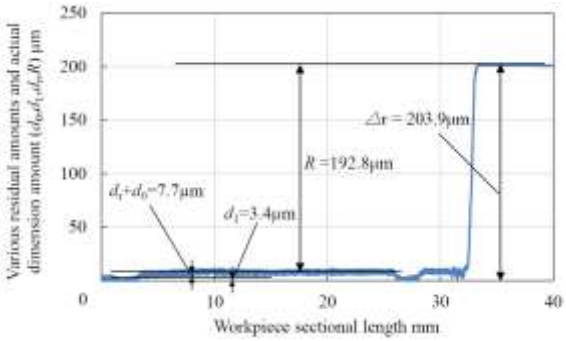

Fig 13 Variations of residual amount and stock removal with SD80Br (Δ_r=203.9μm)

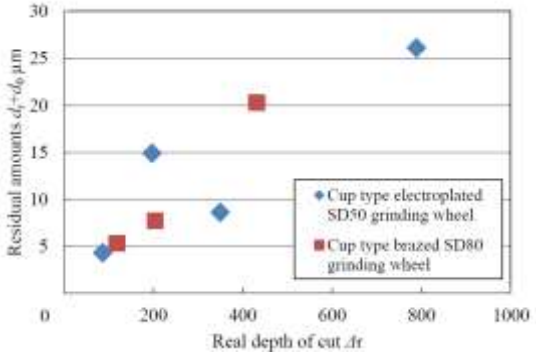

Fig 14 Variations of residual amounts of workpiece

Residual amount and stock removal

Fig 12 shows the cross sectional profile of the workpiece at Δr=349.6μm with SD50P wheel. A grinding wheel wear is d_0, a residual amount due to an elastic deformation of grinding system is d_1(=P/k_{sy}, k_{sy} is a grinding system stiffness), another residual amount is d_r and a real stock removal is R_r. The pre-ground surface height which remain before and after grinding test area adjusted horizontally. An inclination of the grinding test area is almost zero, the wheel wear might be very small. And the amount of the elastic deformation of the grinding system is maintained constant value, because the normal grinding force is constant.

Fig 13 shows the cross sectional profile of the workpiece with the SD80Br wheel at Δ_r=203.9μm. The variations of the residual amounts vary the same way of the Fig 12.

Fig 14 shows the residual amount of the d_0+d_r versus the real setting depth of cut. Although deviation of the amount of the SD50P wheel is occur, it becomes large with the real depth of cut.

Conclusions

In this study, with the two types of the joining method of the grain to the base metal of the cup type wheel, the grinding force, the grinding force distribution and the residual amount are experimentally analysed in the face grinding of the cemented carbide. The experimental parameter is the setting depth of cut, while under the constant feed rate of the wheel head. Main conclusions obtained in this study are as follows.

1) When it is over the setting depth of cut 400μm, the steady grinding state does not appear, and the grinding force becomes larger with the increase of a grinding time.
2) With the increase of the setting depth of cut, the peak value of the grinding force distribution increases, while the peak width almost the same.
3) The coarse diamond grain provides well grinding condition, but it deals large stress to the individual grain, so the drop off of the grain is occurred.

Acknowledgement

This work was supported by JSPS KAKENHI Grand-in-Aid for Scientific Research (C) Grant Number JP26420051.

Reference

[1] M. Saeki, T. Kuriyagawa and K. Syoji, Machining of Aspherical Molding Dies Utilizing Parallel Grinding Method, J. JSPE, 68, 8 (2002) pp.1067-1071.

[2] T. Magara, H. Yamada, S. Sato, T. Yatomi and K. Kobayashi, Improvement of Surface Quality by Non-Electrolysis Wire-EDM, J. JSPE, 59, 7 (1993) pp.1157-1162.

[3] S. Sasaya, N. Takenaka, Study on Grinding Mechanism of Vertical Spindle Surface Grinding : On the Wheel Wear. Journal of the Japan Society of Mechanical Engineers (C), Vol. 46, No. 408 (1980) pp. 979-989.

[4] H. Nakagawa, Y. Kita, Kakino, A. Matsubara, S. Tateiwa, Grinding by Grinding Center : Development of Endmill Type Wheel Base with the Function of Sucking Coolant, Journal of Abrasive Machining, Vol. 39, No. 4 (1995) pp. 194-199.

[5] T. Fujiwara, S. Tsukamoto, K. Ohashi and T. Onishi, Study on Grinding Force Distribution on Cup Type Electroplated Diamond Wheel in Face Grinding of Cemented Carbide, Advances in Abrasive Technology XVII, Advanced Material Research, vol.1017, Trans Tech Publications (2014) p 9-14.

[6] T. TSUJINO, T. FUJIWARA, H. KODAMA, T. ONISHI, S. TSUKAMOTO and K. OHASHI, Influence on Grinding Force Distribution in Feed Rate Variations of Cemented Carbide with Vertical Face Grinding, Proceedings of ISAAT 2019, (2019).